

Reactivity of Trinuclear Ruthenium Clusters with Mercury Halides¹

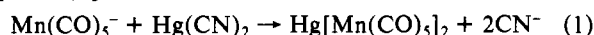
Edward Rosenberg,*† David Ryckman,† I-Nan Hsu,† and Robert W. Gellert†

Received January 2, 1985

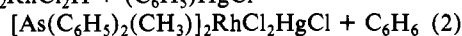
The reactions of $\text{Ru}_3(\text{CO})_{12}$, $\text{HRu}_3(\text{CO})_{11}^-$, and $\text{Ru}(\text{CO})_4^{2-}$ with $\text{IHgRu}_3(\text{CO})_9(\mu_3\text{-C}_2\text{-}t\text{-Bu})$ (II) have been studied. The reaction of II with the above species gives the novel cluster *cis*- $\text{Ru}(\text{CO})_4[\text{HgRu}_3(\text{CO})_9(\mu_3\text{-C}_2\text{-}t\text{-Bu})]_2$ (III), whose solid-state structure has been determined by X-ray diffraction. Compound III crystallizes in the monoclinic space group $P2_1/n$ with $a = 11.534$ (8) Å, $b = 24.456$ (8) Å, $c = 18.160$ (5) Å, $\beta = 108.05$ (4)°, $V = 4870$ (4) Å³, and $d_{\text{calcd}} = 2.574$ g cm⁻³ for $Z = 4$. Least-squares refinement led to final agreement indices of $R_F = 0.045$ and $R_{wF} = 0.059$ for 5586 observed reflections. In the complex the $\text{C}_2\text{-}t\text{-Bu}$ ligand is $\mu_3\text{-}\eta^2$ -bonded to the triruthenium fragments of the molecule as in II. In addition, it is found that $\text{Hg}[\text{Ru}_3(\text{CO})_9(\mu_3\text{-C}_2\text{-}t\text{-Bu})]_2$ (IV) is a major byproduct of the reaction of II with the above ruthenium complexes. The equilibrium constant for the redistribution of $\text{XHgRu}_3(\text{CO})_9(\mu_3\text{-C}_2\text{-}t\text{-Bu})$ ($X = \text{Br}^-$, I^-) to the symmetric species $\text{Hg}[\text{Ru}_3(\text{CO})_9(\mu_3\text{-C}_2\text{-}t\text{-Bu})]_2$ and HgX_2 has been determined. The values obtained for K_{eq} were 0.8 and 0.5 for $X = \text{Br}^-$ and I^- , respectively. Furthermore, $\text{Ru}_3(\text{CO})_{12}$, $\text{HRu}_3(\text{CO})_{11}^-$, and $\text{Ru}(\text{CO})_4^{2-}$ are found to accelerate this redistribution reaction. The subsequent reaction of $\text{Ru}_3(\text{CO})_{12}$ and $\text{HRu}_3(\text{CO})_{11}^-$ with II is thought to take place by oxidative addition of the mercury-iodine bond across the metal-metal bonds of the trinuclear clusters.

Introduction

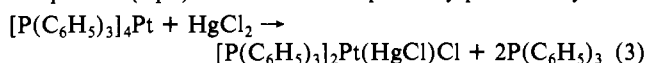
Three pathways have been found to dominate the reactions of mercuric halides and organomercuric halides with low-valent transition-metal complexes. The most common is the reaction of a metal carbonyl anion with a mercury halide or pseudohalide compound (eq 1).^{2a} A second is the reaction of a metal hydride



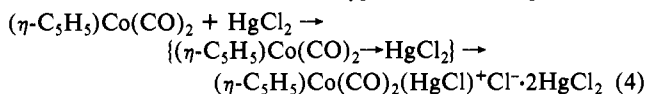
species with an alkyl- or arylmercuric halide (eq 2).^{2b} In this $[\text{As}(\text{C}_6\text{H}_5)_2\text{CH}_3]_2\text{RhCl}_2\text{H} + (\text{C}_6\text{H}_5)\text{HgCl} \rightarrow$



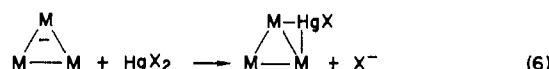
reaction the metal hydride may be considered to be a protonated metal anion, which serves to electrophilically cleave the mercury-carbon bond. A third mode of reaction is the oxidative addition of the mercury-halogen bond to low-valent neutral transition-metal compounds (eq 3).³ This reaction probably proceeds by a dis-



sociative mechanism in which tetrakis(triphenylphosphine)platinum, an 18-electron compound, loses two phosphine ligands and adds chloride and the HgCl group to form a 16-electron platinum(II) complex. In a few cases isolation of a Lewis acid-base adduct is possible (eq 4), and this type of adduct may be a primary intermediate in reactions of the type illustrated (eq 1 and 3).⁴

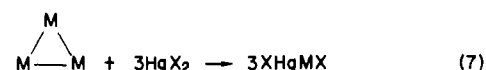


When the reactions of low-valent metal cluster complexes with mercuric halides are considered, novel but related reaction pathways would be possible. Halide displacement could yield two types of product: (1) a terminal mercury cluster linkage with a two-center two-electron transition-metal-mercury bond (eq 5); (2) an edge-bridged linkage with a three-center two-electron mercury transition metal bond (eq 6).

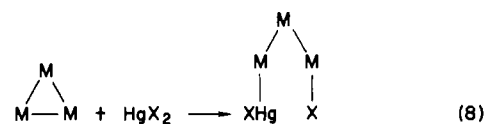


In polynuclear compounds the negative charge is likely to be delocalized over two or more metal centers, and the latter would be expected by analogy with H^+ . Indeed we and others have found

that eq 6 is the preferred pathway. For example, when $[\text{As}(\text{C}_6\text{H}_5)_4]^+[\text{Ru}_3(\text{CO})_9(\mu_3\text{-C}_2\text{-}t\text{-Bu})]^-$ (I) reacts with mercuric halide, the product, $\text{XHgRu}_3(\text{CO})_9(\mu_3\text{-C}_2\text{-}t\text{-Bu})$ (II) ($X = \text{Br}^-$, I^-), contains a bridged three-center two-electron mercury-ruthenium bond.^{6,7} However, in compound I the organic ligand may play an important role in holding the metal framework together, thus directing the course of the reaction toward halide displacement. For neutral and anionic trinuclear clusters not bridged by heteroatoms, oxidative addition of the mercuric halide, leading to fragmentation of the cluster, could be an alternative reaction pathway occurring in one of two ways: (1) the mercuric halide could add to a single metal center and, in the presence of excess mercuric halide, give 3 equiv of XHgMX (eq 7); (2) the



mercuric halide could add across a metal-metal bond to give a mercury-metal bond and a transition-metal-halogen bond on two different metal atoms (eq 8). Further oxidative addition of the



mercuric halide, cleaving the remaining metal-metal bonds, could lead to the same product as in eq 7 or products of the type $\text{M}(\text{HgX})_2$ and M_2X_2 . We report here the results of our studies on the reaction of II with the trinuclear ruthenium clusters $\text{Ru}_3(\text{CO})_{12}$ and $\text{HRu}_3(\text{CO})_{11}^-$, which shed some light on the relationship between these alternative reaction pathways (eq 7 and 8).

Results and Discussion

A. Reaction of II with $\text{Ru}_3(\text{CO})_{12}$. When 2 equiv of II is reacted with 1 equiv of $\text{Ru}_3(\text{CO})_{12}$ in THF or chloroform, one major product, *cis*- $\text{Ru}(\text{CO})_4[\text{HgRu}_3(\text{CO})_9(\mu_3\text{-C}_2\text{-}t\text{-Bu})]_2$ (III), was isolated and purified. In addition, $\text{Hg}[\text{Ru}_3(\text{CO})_9(\mu_3\text{-C}_2\text{-}t\text{-Bu})]_2$

- (1) Taken in part from: Ryckman, D. Masters Thesis, California State University Northridge, CA, 1983.
- (2) (a) Hieber, W.; Schropp, W., Jr. *Chem. Ber.* **1960**, *93*, 455. (b) Nyholm, R. S.; Vrieze, K. *J. Chem. Soc., Dalton Trans.* **1965**, 5331.
- (3) Layton, A. J.; Nyholm, R. S.; Pneumatikakis, G. A.; Tobe, M. L. *Chem. Ind. (London)* **1967**, 465.
- (4) Nowell, I. W.; Russell, D. R. *J. Chem. Soc., Dalton Trans.* **1965**, 5331.
- (5) Mays, M. J.; Robb, J. D. *J. Chem. Soc., Dalton Trans.* **1968**, 329.
- (6) King, K.; Rosenberg, E.; Tiripicchio, A.; Tiripicchio-Camellini, M. *J. Am. Chem. Soc.* **1980**, *102*, 3626.
- (7) Rosenberg, E.; Hardcastle, K. I.; Tiripicchio, A.; Tiripicchio-Camellini, M.; Ermer, S. E.; King, K. *Inorg. Chem.* **1983**, *22*, 1339.

* California State University, Northridge.

† California State University, Los Angeles.

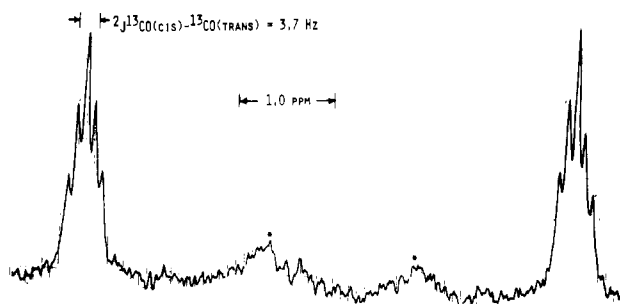


Figure 1. ^{13}C NMR spectrum of the carbonyl region of *cis*-(^{13}CO) $_4\text{Ru}$ -[$\text{HgRu}_3(\text{CO})_9(\mu_3\text{-C}_2\text{-}t\text{-Bu})$] $_2$ (III) in THF at room temperature. An asterisk denotes natural-abundance exchange-broadened ^{13}CO resonances on Ru_3 clusters.

Table I. Selected Bond Lengths (Å) of *cis*- $\text{Ru}(\text{CO})_4[\text{HgRu}_3(\text{CO})_9(\mu_3\text{-C}_2\text{-}t\text{-Bu})]_2$ (III)

Hg(1)–Ru(7)	2.658 (1)	Hg(2)–Ru(7)	2.655 (1)
Hg(1)–Ru(1)	2.810 (1)	Hg(2)–Ru(5)	2.791 (1)
Hg(1)–Ru(2)	2.833 (1)	Hg(2)–Ru(4)	2.844 (1)
Ru(1)–Ru(2)	2.857 (1)	Ru(4)–Ru(5)	2.873 (1)
Ru(1)–Ru(3)	2.810 (1)	Ru(4)–Ru(6)	2.794 (1)
Ru(2)–Ru(3)	2.803 (2)	Ru(5)–Ru(6)	2.799 (2)
Ru(7)–C(71)	1.92 (2)	C(71)–O(71)	1.15 (2)
Ru(7)–C(72)	1.90 (2)	C(72)–O(72)	1.12 (2)
Ru(7)–C(73)	1.90 (2)	C(73)–O(73)	1.14 (2)
Ru(7)–C(74)	1.94 (2)	C(74)–O(74)	1.11 (2)

(IV) is formed from the redistribution of the unsymmetrical compound II.^{6,7} The new compound apparently arises from oxidative addition to the metal–metal bonds of $\text{Ru}_3(\text{CO})_{12}$.

The formula of III was deduced by ^1H and ^{13}C NMR spectroscopy and elemental analysis. A single-crystal X-ray analysis of III confirmed the proposed structure and will be discussed in the following section. The ^1H NMR spectrum of III in CD_2Cl_2 consists only of a singlet at 1.37 ppm attributed to the protons of the *tert*-butyl group. The two sets of protons are apparently equivalent as a result of rotation about the central ruthenium–mercury bonds even though the two *tert*-butyl groups are not equivalent in the solid state.

The reaction of II with ^{13}C -enriched $\text{Ru}_3(\text{CO})_{12}$ was also followed by ^{13}C NMR spectroscopy. As the reaction progressed, the intensity of the single resonance at 199.47 ppm, due to the carbonyls of $\text{Ru}_3(\text{CO})_{12}$, gradually decreased in intensity as four new peaks at 202.85, 197.70, 198.55, and 198.09 ppm appeared. When all of the $\text{Ru}_3(\text{CO})_{12}$ was consumed, the two sets of new peaks integrated 1:2. The resonances at 198.55 and 198.09 ppm are tentatively assigned to the coproduct of cluster cleavage, which is produced on the formation of III but which has not been fully characterized yet. Chromatographic separation of the reaction mixture yielded orange crystals of III. The ^{13}C NMR spectrum of isolated III showed it to be stereochemically rigid at the central Ru atom with two signals at 202.85 and 197.70 ppm due to the carbonyl ligands *cis* and *trans* to the mercury atoms, showing the expected ^{13}CO – ^{13}CO coupling pattern (Figure 1).

B. Crystal Structure of *cis*- $\text{Ru}(\text{CO})_4[\text{HgRu}_3(\text{CO})_9(\mu_3\text{-C}_2\text{-}t\text{-Bu})]_2$. The X-ray diffraction analysis of III shows the molecule to be a slightly distorted octahedron with four carbon monoxide ligands and two *cis*- $\text{HgRu}_3(\text{CO})_9(\mu_3\text{-C}_2\text{-}t\text{-Bu})$ fragments bound to a central ruthenium atom, Ru(7) (Figure 2). Tables I and II list some selected bond distances and angles. Both mercury–central ruthenium atom bonds Hg(1)–Ru(7) and Hg(2)–Ru(7) are 2.66 Å. The Hg(1)–Ru(7)–Hg(2) bond angle is unusually small (84°). The intramolecular nonbonding Hg(1)–Hg(2) distance is 3.55 Å. The shortness of this nonbonded contact suggests that there may be significant Hg(1)–Hg(2) interaction, which causes the unusually small bond angle of 84° between the *cis*-mercury atoms. This Hg(1)–Hg(2) interaction is more pronounced for *cis*- $\text{Fe}(\text{CO})_4(\text{HgBr})_2$, which is a dimer in the solid state.⁸ The iron–mercury bond lengths are 2.42 and 2.59 Å while

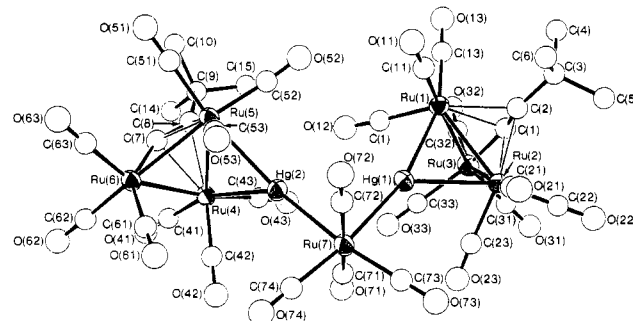


Figure 2. ORTEP illustration of *cis*- $\text{Ru}(\text{CO})_4[\text{HgRu}_3(\text{CO})_9(\mu_3\text{-C}_2\text{-}t\text{-Bu})]_2$ (III) showing the approximate octahedral geometry around the central ruthenium atom Ru(7).

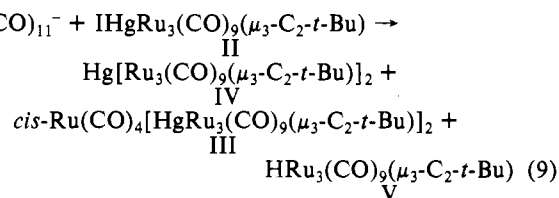
Table II. Selected Bond Angles (deg) of *cis*- $\text{Ru}(\text{CO})_4[\text{HgRu}_3(\text{CO})_9(\mu_3\text{-C}_2\text{-}t\text{-Bu})]_2$ (III)

Angles around Mercury			
Ru(7)–Hg(1)–Ru(1)	163.47 (4)	Ru(7)–Hg(2)–Ru(5)	153.84 (4)
Ru(7)–Hg(1)–Ru(2)	134.37 (4)	Ru(7)–Hg(2)–Ru(4)	141.20 (4)
Ru(7)–Hg(1)–Ru(2)	60.83 (3)	Ru(5)–Hg(2)–Ru(4)	61.30 (3)
Angles around Octahedrally Disposed Ruthenium			
C(73)–Ru(7)–C(72)	97.7 (7)	C(72)–Ru(7)–C(71)	167.6 (7)
C(73)–Ru(7)–C(71)	94.6 (8)	C(72)–Ru(7)–C(74)	94.0 (7)
C(73)–Ru(7)–C(74)	101.7 (8)	C(72)–Ru(7)–Hg(2)	87.5 (5)
C(73)–Ru(7)–Hg(2)	170.3 (6)	C(72)–Ru(7)–Hg(1)	85.8 (5)
C(73)–Ru(7)–Hg(1)	86.8 (6)	C(71)–Ru(7)–C(74)	92.1 (7)
C(71)–Ru(7)–Hg(2)	82.0 (5)	C(71)–Ru(7)–Hg(1)	86.5 (5)

the Hg(1)–Hg(2) angle is 81° . This causes a corresponding decrease in the Hg(1)–Hg(2) intramolecular distance to 3.1 Å.

It should also be noted that the bridged-ruthenium–ruthenium and the ruthenium–mercury distances are almost the same for III (2.86, 2.82 Å) and IV (2.84, 2.82 Å).⁷ Thus, the overall coordination number around mercury is not a critical factor in the determination of these bond lengths in this family of complexes, but the overall electronegativity of the groups attached to mercury is (i.e., compare distances in II (2.90, 2.73 Å) with those in III and IV above). As expected, the two-center two-electron bonds in III are significantly shorter (2.66 Å) than the μ -Hg–Ru interactions. The metal–carbon distances and angles in the Ru_3 clusters in III are essentially the same as in II and IV.

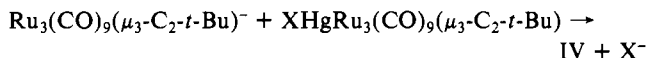
C. Reaction of II with $[\text{N}(\text{C}_2\text{H}_5)_4][\text{HRu}_3(\text{CO})_{11}]$. When the anionic cluster species, $\text{HRu}_3(\text{CO})_{11}^-$, was combined with II in THF under nitrogen, three products were isolated from the silica gel TLC workup (eq 9). A base line material was also obtained,



but was not fully characterized. This material had the same carbonyl stretching region in the IR spectrum as the base line material obtained when $\text{Ru}_3(\text{CO})_{12}$ was reacted with II.

As noted by TLC, IV forms immediately. Evidently the redistribution is even more facile with the anionic cluster than with $\text{Ru}_3(\text{CO})_{12}$, where IV forms more slowly. Perhaps the electron-rich cluster provides an even better site to which two molecules of IV may coordinate. The presence of $\text{HRu}_3(\text{CO})_9(\mu_3\text{-C}_2\text{-}t\text{-Bu})^-$ (V), isolated and identified by ^1H NMR, can be explained by proton transfer from $\text{HRu}_3(\text{CO})_{11}^-$ to $\text{Ru}_3(\text{CO})_9(\mu_3\text{-C}_2\text{-}t\text{-Bu})^-$ generated upon dissolution of the unsymmetrical mercuric compound II. This process may also contribute to the faster consumption of starting materials and the rapid formation of IV by the reaction

(8) Baird, H. W.; Dahl, L. F. *J. Organomet. Chem.* **1967**, *7*, 503.



A 25% yield of the oxidative-addition product, III, was obtained.

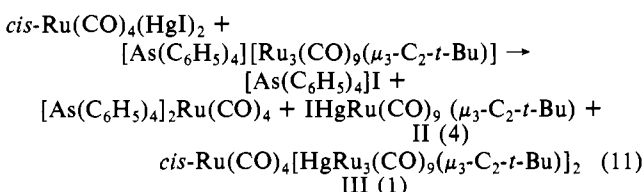
D. Reaction of $[\text{N}(\text{C}_2\text{H}_5)_4]\text{HRu}_3(\text{CO})_{11}$ with HgI_2 . When 1, 2, or 3 equiv of HgI_2 are reacted with $[\text{N}(\text{C}_2\text{H}_5)_4]\text{HRu}_3(\text{CO})_{11}$, increasingly larger amounts of a yellow insoluble compound precipitated from the solution. This precipitate VI contains no halogen and has a mercury, ruthenium, and carbon analysis consistent with the empirical formula $\text{HgRu}(\text{CO})_4$. It has four infrared bands (see Experimental Section) consistent with C_{2v} symmetry expected for an $[\text{HgRu}(\text{CO})_4]_n$ polymer where the mercury atoms are cis as in III. It is possible that reduction of products analogous to III takes place in the presence of the electron-rich cluster $\text{HRu}_3(\text{CO})_{11}^-$. The compound is completely insoluble in all common organic solvents but gave consistent infrared and elemental analysis. Yields of 50–60% are consistently obtained on the basis of conversion of $\text{HRu}_3(\text{CO})_{11}^-$ to three $\text{HgRu}(\text{CO})_4$, and no unreacted $\text{Ru}_3(\text{CO})_{12}$ was found in the reaction supernatant. Some unreacted $\text{Ru}_3(\text{CO})_{12}$ is found in the reactions with 1 or 2 equiv of HgI_2 .

E. Reaction of $\text{Na}_2\text{Ru}(\text{CO})_4$ with $\text{IHgRu}_3(\text{CO})_9(\mu_3\text{-C}_2\text{-}t\text{-Bu})$. In an attempt to find a high-yield synthesis of III, $\text{Na}_2\text{Ru}(\text{CO})_4$ was reacted with II in THF at 0 °C. It was hoped that the reaction would be rapid and give little or no redistribution to IV. As indicated by TLC, the reaction is immediate; all of II is consumed within 5 min. After chromatographic separation of the reaction mixture, two isolable products and a red base line material are obtained (eq 10). An 18% yield of III is isolated. This low yield $\text{Na}_2\text{Ru}(\text{CO})_4 + \text{IHgRu}_3(\text{CO})_9(\mu_3\text{-C}_2\text{-}t\text{-Bu}) \rightarrow$

$$\begin{array}{l} \text{cis-Ru}(\text{CO})_4[\text{HgRu}_3(\text{CO})_9(\mu_3\text{-C}_2\text{-}t\text{-Bu})]_2 + \\ \text{III (18\%)} \\ \text{Hg}[\text{Ru}_3(\text{CO})_9(\mu_3\text{-C}_2\text{-}t\text{-Bu})]_2 \text{ (IV)} \\ \text{IV (40\%)} \end{array} \quad (10)$$

may be due to the presence of $\text{HRu}(\text{CO})_4^-$ and volatile $\text{H}_2\text{Ru}(\text{CO})_4$ as contaminants present in $\text{Na}_2\text{Ru}(\text{CO})_4$. Again it was noted that redistribution was facile, and a 40% yield of IV is obtained. The presence of a cluster is thus not necessary for the formation of III, but the more nucleophilic mononuclear anion gives more IV than III while the opposite is true for the reactions of II with $\text{HRu}_3(\text{CO})_{11}^-$.

It is apparent that a high-yield synthesis of III has to exclude II as a reactant since this compound readily forms IV in the presence of the necessary coreactants. Therefore, $\text{cis-Ru}(\text{CO})_4(\text{HgI})_2$, which may be prepared in 90% yield from $\text{Ru}_3(\text{C-O})_{12}$ and HgI_2^{9a} was reacted with I. It was hoped that the mildly nucleophilic $\text{Ru}_3(\text{CO})_9(\mu_3\text{-C}_2\text{-}t\text{-Bu})^-$ fragment would displace iodide from $\text{cis-Ru}(\text{CO})_4(\text{HgI})_2$ to yield III without the formation of IV. The reaction progress was followed by ^1H NMR. The major products formed were III and II in a ratio of 1:4 (eq 11).



In addition, a small amount of IV was also formed. The metal–mercury bond is thus more readily cleaved than the mercury–halogen bond.

The coproduct from the Ru–Hg bond cleavage would be $[\text{As}(\text{C}_6\text{H}_5)_4]_2\text{Ru}(\text{CO})_4$, which was not isolated, but the presence of $\text{Ru}(\text{CO})_4^{2-}$ was detected by IR spectroscopy of the NMR samples. Here again as in the formation of III and IV from II, the reaction path of a common Ru–Hg intermediate (presumably an acid–base complex between Ru_3^- and $\text{cis-Ru}(\text{CO})_4(\text{HgI})_2$) is

partitioned between the products II and III. Product II results from Ru–Hg cleavage and product III from two Hg–I bond cleavages.

F. Determination of the Redistribution Equilibria for $\text{XHgRu}_3(\text{CO})_9(\mu_3\text{-C}_2\text{-}t\text{-Bu})$ ($\text{X} = \text{Br}^-, \text{I}^-$). We have previously suggested that IV and HgX_2 arise from the redistribution of halomercuric compounds of the form $\text{XHgRu}_3(\text{CO})_9(\mu_3\text{-C}_2\text{-}t\text{-Bu})$ ($\text{X} = \text{Cl}^-, \text{Br}^-, \text{I}^-$) in THF (eq 12); however, no quantitative

$$2\text{XHgRu}_3(\text{CO})_9(\mu_3\text{-C}_2\text{-}t\text{-Bu}) \rightarrow \text{Hg}[\text{Ru}_3(\text{CO})_9(\mu_3\text{-C}_2\text{-}t\text{-Bu})]_2 + \text{HgX}_2 \quad (12)$$

measurements were made.⁹ We report here the room-temperature solution-phase redistribution of the asymmetric bromo- and iodomercuric derivatives to IV and HgX_2 in CDCl_3 . The reaction progress was monitored by ^1H NMR spectroscopy. The original singlet at 1.34 ppm due to the methyl groups on II decreased, and a new singlet at 1.50 ppm attributable to the methyl groups on IV increased. When no further change in the integration ratio of the symmetric to the asymmetric species was observed, the reaction was assumed to be at equilibrium. The formation of HgX_2 was assumed, as no attempts were made to isolate this product. The relative concentrations were determined from the integration and the equilibrium constant calculated from the reaction stoichiometry as follows:



where $\text{X} = \text{Br}^-, \text{I}^-$ and $\text{A} = \text{Ru}_3(\text{CO})_9(\mu_3\text{-C}_2\text{-}t\text{-Bu})^-$

$$K_{\text{eq}} = \frac{[\text{HgA}_2][\text{HgX}_2]}{[\text{XHgA}]^2}$$

Since $[\text{HgA}_2] = [\text{HgX}_2]$ at equilibrium, the equilibrium expression may be written as

$$K_{\text{eq}} = \frac{[\text{HgA}_2]^2}{[\text{XHgA}]^2}$$

The values obtained for the redistribution equilibrium constants by this method are 0.5 when $\text{X} = \text{I}^-$ and 0.8 when $\text{X} = \text{Br}^-$. Entropy considerations alone would tend to favor the unsymmetrical compound (II) in this equilibrium. Compounds containing two-center two-electron mercury–transition-metal bonds usually give very small K_{eq} values for eq 12 as written. In IV, however, additional delocalization of electron density in the larger metal framework could account for its unusual stability relative to II. Involvement of more 6p orbital character in the bonds of Hg in the three-coordinate II would favor further expansion of the coordination sphere of the mercury atom by lowering the mercury valence bond promotion energy for adopting coordination number four; this may also contribute to the special stability of IV. The fact that II is a bridged dimer in the solid state is consistent with this idea. Since the energy of the Hg–Br bond in HgBr_2 is greater than the energy of Hg–I bond in HgI_2 , one would expect the equilibrium constant to be greater for the bromide (II), as observed. As a result of this redistribution, IV will always be formed when an unsymmetric mercury-containing compound such as II is used as a reactant.

G. Promotion of the Redistribution Reaction by Ru_3 Clusters. During the reaction of $\text{Ru}_3(\text{CO})_{12}$ and $\text{HRu}_3(\text{CO})_{11}^-$ with $\text{IHgRu}_3(\text{CO})_9(\mu_3\text{-C}_2\text{-}t\text{-Bu})$, it was noted that $\text{Ru}_3(\text{CO})_{12}$ or $\text{HRu}_3(\text{CO})_{11}^-$ accelerated the redistribution reaction. A study was made on the effect of $\text{Ru}_3(\text{CO})_{12}$ concentration on the rate of formation of IV. The redistribution reaction took 30 days to reach equilibrium in CDCl_3 when no other metal species was present. The effect of $\text{Ru}_3(\text{CO})_{12}$ concentration on the time to reach equilibrium was dramatic, as equilibrium was approached in several hours, at which time III began to form in appreciable amounts as observed by ^1H NMR. In our experiments the concentration of $\text{Ru}_3(\text{CO})_{12}$ was varied while the concentration of II was held constant. The amount of IV formed was measured by the intensity of the ^1H NMR signal after a 1-h reaction time. This short time interval was chosen in order to avoid errors in measuring the concentration of II due to its reaction with Ru_3^-

(9) (a) Ryckman, D. Master's Thesis, California State University, Northridge, CA, 1983. (b) King, K. Master's Thesis, California State University, Northridge, CA, 1982.

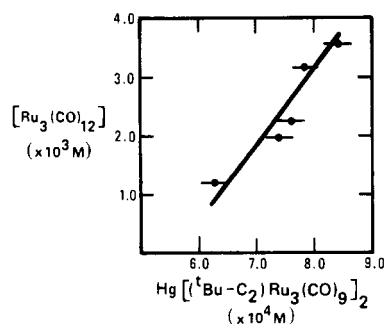


Figure 3. Concentration of $\text{Hg}[\text{Ru}_3(\text{CO})_9(\mu_3\text{-C}_2\text{-}t\text{-Bu})_2]$ (IV) obtained from $\text{BrHg}[\text{Ru}_3(\text{CO})_9(\mu_3\text{-C}_2\text{-}t\text{-Bu})]$ (IIa) vs. $\text{Ru}_3(\text{CO})_{12}$ concentration after 1 h of reaction time at room temperature.

(CO)₁₂ to form III. We observe a linear dependence of the rate of formation of IV on $\text{Ru}_3(\text{CO})_{12}$ in the concentration range examined (Figure 3), which suggests the rate law $d[\text{IV}]/dt = [\text{II}]^n[\text{Ru}_3(\text{CO})_{12}]$ where $n = 1$ or 2. The straight-line plot does not pass through zero since the uncatalyzed reaction would undoubtedly proceed by a different mechanism. This mechanism could have a first-order (dissociative) or a second-order (four-center transition state) dependence on II. Our main point here is that electron-rich metal centers such as $\text{Ru}_3(\text{CO})_{12}$, $\text{HRu}_3(\text{CO})_{11}^-$, and $\text{Ru}(\text{CO})_4^{2-}$ promote this redistribution by formation of a donor-acceptor complex with the electrophilic mercury center in II.

Conclusions

There is a sharp contrast between the reaction of II with $\text{Ru}_3(\text{CO})_9(\mu_3\text{-C}_2\text{-}t\text{-Bu})^-$ and its reaction with $\text{Ru}_3(\text{CO})_{12}$ or $\text{HRu}_3(\text{CO})_{11}^-$. In the case of $\text{Ru}_3(\text{CO})_{12}$ and $\text{HRu}_3(\text{CO})_{11}^-$, products that are the result of oxidative addition are formed while with $\text{Ru}_3(\text{CO})_9(\mu_3\text{-C}_2\text{-}t\text{-Bu})^-$ halide displacement occurs to give a $\mu\text{-Hg-Ru}$ bond. This difference in reaction pathways is probably due to the presence of the organic ligand ($\mu_3\text{-C}_2\text{-}t\text{-Bu}$), which holds the triangular ruthenium framework together. A similar result is observed when $(\mu\text{-H})_2(\mu_3\text{-S})\text{Ru}_3(\text{CO})_9$ reacts with the Lewis acid SnCl_4 .¹⁰ In this case, one of the Ru-Ru bonds is cleaved with loss of CO. The lost metal-metal bond is replaced with a bridging chloride to give $(\mu\text{-H}_2)(\mu_3\text{-S})(\mu\text{-Cl})\text{Ru}_3(\text{CO})_9\text{SnCl}_3$. This pathway also contrasts with the reaction of $\text{Ru}_3(\text{CO})_{12}$ with SnCl_4 , which yields $\text{Ru}_3(\text{CO})_{12}\text{Cl}(\text{SnCl}_3)$,¹² a linear chain of metals like $\text{Os}_3(\text{CO})_{12}\text{I}_2$.¹³ In all of the reactions involving II, it was found that this unsymmetric mercury compound redistributes to the symmetric species IV and HgI_2 . The equilibrium slightly favors IV in the cases examined quantitatively. This contrasts sharply with most two-center- two-electron-bonded transition-metal mercury compounds, where the equilibrium for redistribution favors the unsymmetric species.¹⁴ The formation of two three-center two-electron bonds in one molecule apparently results in additional thermodynamic stability in IV when compared with II.

It was also found that $\text{Ru}_3(\text{CO})_{12}$ promotes these redistribution reactions. It seems reasonable that a Lewis acid-base complex plays a role in the observed catalysts by bringing two molecules of II into close proximity. Complexation of II with $\text{Ru}_3(\text{CO})_{12}$ could also promote dissociation of X^- (Br^- , I^-). The complexation of II with Ru_3 clusters appears to be directly related to its subsequent reactions with these species. Finally, the results reported here for the reaction of $\text{HRu}_3(\text{CO})_{11}^-$ with Hg^{2+} salts are in sharp contrast to the recent results reported for the osmium analogue, $\text{HOs}_3(\text{CO})_{11}^-$, where the integrity of the cluster is preserved and a trimeric mercury-bridged cluster ($\text{HgOs}_3(\text{CO})_{11}$)₃ is obtained.¹⁵

This difference is undoubtedly due to the stronger Os-Os bond when compared with the Ru-Ru bond of the ruthenium analogue.

Experimental Section

General Comments. Reactions were performed in standard Schlenkware. The apparatus was flame-dried in vacuo and refilled with carbon monoxide or nitrogen; manipulations were performed under an atmosphere of nitrogen or carbon monoxide except the thin-layer chromatography.

Materials. Mercuric iodide was from MCB. $\text{Ru}_3(\text{CO})_{12}$ was synthesized by literature methods from $\text{RuCl}_3 \cdot 3\text{H}_2\text{O}$;¹³ $\text{Na}_2\text{Ru}(\text{CO})_4$,¹¹ $\text{HRu}_3(\text{CO})_{11}^-$,¹⁶ $\text{HRu}_3(\text{CO})_9(\mu_3\text{-C}_2\text{-}t\text{-Bu})$,⁷ and II⁷ were prepared by published methods from $\text{Ru}_3(\text{CO})_{12}$.¹⁵

Solvents. Solvents were transferred by cannula or syringe. THF was distilled under nitrogen prior to use from sodium benzophenone ketyl. 2-Ethoxyethanol, previously dried over magnesium sulfate, was distilled in air, thoroughly degassed, saturated with carbon monoxide, and used immediately. Other solvents were stored over molecular sieves (4 Å) and saturated with nitrogen before use.

Spectra. Both solution (CHCl_3 and CH_2Cl_2) and potassium bromide pellet infrared spectra were recorded on a Beckman IR 20A-X spectrophotometer. ¹H NMR spectra were measured in CD_2Cl_2 or CDCl_3 , which was used as an internal reference (5.32 or 7.24 ppm). ¹³C NMR spectra were taken in THF with 10% THF-*d*₆ or CDCl_3 added to obtain a lock. The THF signals at 86.7 and 25.3 ppm or the CDCl_3 signal at 77.0 ppm relative to Me_4Si were used as references. NMR data were acquired on an IBM NR/80 spectrometer. ¹³C NMR samples were taken of solutions of 30–40% ¹³CO-enriched $\text{Ru}_3(\text{CO})_{12}$. The solutions were made 0.04 M in $\text{Cr}(\text{acac})_3$ (*acac* = acetylacetonate) prior to examination.

Analysis. Carbon and hydrogen analyses were performed by Schwarzkopf Microanalytical Laboratories, Woodside, NY. Metal analyses (Hg, Ru) were done by neutron activation analysis. Samples of 5–10 mg were weighed to the nearest thousandth of a milligram into polyethylene vials and sealed under nitrogen. Standards and samples were then irradiated for 5 min in a thermal neutron flux of 10^{12} neutrons/cm² and counted at the nuclear reactor facility at the University of California, Irvine. Calculations for percentage of metals in each sample were done by using standard equations for activity and decay corrections at California State University, Northridge, with the aid of a computer.

Preparation of III by Reaction of $\text{Ru}_3(\text{CO})_{12}$ with II. $\text{Ru}_3(\text{CO})_{12}$ (50.0 mg, 0.078 mmol) was dissolved in THF (20.0 mL) with stirring. To the resultant solution was added II (150 mg, 0.156 mmol) in THF (10.0 mL) by syringe. The reaction mixture was stirred at room temperature under nitrogen for 4 days when the original yellow-orange solution became deep red. The THF was removed by trap to trap distillation, leaving a red residue. The reaction residue was dissolved in a minimum amount of dichloromethane and chromatographed on activated silica plates (12). At least five elutions in dichloromethane/hexane (1:4) were necessary to resolve three components and a baseline. Each product was recrystallized from a dichloromethane/hexane mixture at -20°C . Unreacted $\text{Ru}_3(\text{CO})_{12}$ (R_f 0.90; 7.5 mg, 1.2×10^{-2} mmol, 15.5%) was identified by comparison TLC and IR spectroscopy. Compound IV (R_f 0.60; 34.1 mg, 0.0231 mmol, 29.6%) was characterized by comparison TLC and IR and ¹H NMR spectroscopy. Orange crystals of III (R_f 0.50; 16.4 mg, 8.69×10^{-3} mmol, 11.1%) were identified by IR and ¹H NMR: (CDCl_3) 1.39 ppm (s); (CH_2Cl_2) 1.37 ppm (s). Anal. Calcd for *cis*- $\text{Ru}(\text{CO})_4\text{-}[\text{HgRu}_3(\text{CO})_9(\mu_3\text{-C}_2\text{-}t\text{-Bu})_2]$: C, 21.64; H, 0.95; Ru, 37.48; Hg, 21.26. Found: C, 21.52; H, 1.08; Ru 37.00; Hg, 23.01. The oily base line material (47.6 mg) had terminal CO stretching frequencies in the IR and was not further characterized. IR (CH_2Cl_2): 2050 (s), 2025 (s), 2000 (s), 1970 (m) cm^{-1} .

Reaction of II with ¹³C-enriched $\text{Ru}_3(\text{CO})_{12}$ produced *cis*- $\text{Ru}(\text{CO})_4\text{-}[\text{HgRu}_3(\text{CO})_9(\mu_3\text{-C}_2\text{-}t\text{-Bu})_2]$ (III), and the base line material in similar yields. ¹³C NMR spectra were obtained on the two enriched products in the presence of $\text{Cr}(\text{acac})_3$. ¹³C NMR (III, CDCl_3): 202.85 (s), 197.70 (s) ppm.

Preparation of III by Reaction of $[\text{N}(\text{C}_2\text{H}_5)_4][\text{HRu}_3(\text{CO})_{11}]$ with II. To a Schlenk tube containing a solution of II (262 mg, 0.272 mmol) and THF (20.0 mL) at 0°C was added a solution of $[\text{N}(\text{C}_2\text{H}_5)_4][\text{HRu}_3(\text{CO})_{11}]$ (100.8 mg, 0.136 mmol) in THF (10.0 mL) dropwise for 1 h under nitrogen. The original yellow solution became deep red. As indicated by TLC, the reaction was complete after 90 min. The reaction volatiles were removed by trap to trap distillation, leaving a red residue, which

(10) Adams, R. D.; Katahira, D. A. *Organometallics* **1982**, *1*, 53.
 (11) Pomeroy, R. K.; Elder, M.; Hall, D.; Graham, W. A. G. *J. Chem. Soc. A* **1969**, 381.
 (12) Cook, N.; Smart, L.; Woodward, P. *J. Chem. Soc., Dalton Trans.* **1974**, 1744.
 (13) $\text{Ru}_3(\text{CO})_{12}$ preparation from: *Inorg. Synth.* **1976**, *16*, 47.
 (14) Cotton, J. D.; Bruce, M. I.; Stone, F. G. A. *J. Chem. Soc. A* **1968**, 2162.

(15) Fajardo, M.; Holden, H. D.; Johnson, B. F. G.; Lewis, J.; Raithby, P. R. *J. Chem. Soc. Chem. Commun.* **1984**, 24.
 (16) Eady, C. R.; Johnson, B. F. G.; Lewis, J. *J. Chem. Soc., Dalton Trans.* **1978**, 1358.

Table III. Equilibrium Constant Determination for $\text{IHgRu}_3(\text{CO})_9(\mu_3\text{-C}_2\text{-}t\text{-Bu})$ (II)

run 1		run 2	
time, days	integration ratio (IV:II)	time, days	integration ratio (IV:II)
1	0.06	1	0.13
9	1.18	3	0.75
10	1.22	6	0.94
11	1.35	8	1.10
18	1.52	12	1.30
27	1.62	20	1.34
28	1.55	28	1.36
29	1.51	29	1.45
31	1.53	30	1.41

Table IV. Equilibrium Constant Determination by ^1H NMR for $\text{BrHgRu}_3(\text{CO})_9(\mu_3\text{-C}_2\text{-}t\text{-Bu})$ (IIa)

time, days	integration ratio (IV:IIa)	time, days	integration ratio (IV:IIa)
1	0.28	13	1.83
1.5	0.40	20	2.10
7	1.45	21	2.06
9	1.64		

Table V. Effect of $[\text{Ru}_3(\text{CO})_{12}]$ on Redistribution Reaction of $\text{IHgRu}_3(\text{CO})_9(\mu_3\text{-C}_2\text{-}t\text{-Bu})$ (II)

$10^3[\text{Ru}_3(\text{CO})_{12}]$ initially, M	$10^4[\text{IV}]$ after 1 h, M
1.20	6.33
2.00	7.45
2.52	7.54
3.15	7.88
3.78	8.44

was chromatographed as above. In addition to a base line, three bands due to III, IV, and V were isolated and recrystallized as above. The formation of V (R_f 0.95; 57.1 mg, 8.96×10^2 mmol, 32.9%) was shown by comparative TLC and IR and ^1H NMR spectroscopy. The red base line was not crystalline but did contain terminal CO groups. IR (CH_2Cl_2): 2050 (s), 2025 (s), 2000 (s), 1970 (m) cm^{-1} .

Preparation of III by Reaction of $\text{Na}_2\text{Ru}(\text{CO})_4$ with II. Compound II (50.0 mg, 0.052 mmol) was dissolved in THF (10.0 mL) in a Schlenk tube under nitrogen at -38°C . A solution of $\text{Na}_2\text{Ru}(\text{CO})_4$ (6.4 mg, 2.51×10^{-2} mmol) in THF (5.0 mL) was added while the mixture was stirring. As indicated by color change and TLC, reaction occurred instantaneously. The solvent was removed by trap to trap distillation, leaving a red oil, which was dissolved in dichloromethane and chromatographed as above. Three bands were obtained in addition to a heavy base line. The formation of IV (R_f 0.60; 15.2 mg, 1.03×10^{-2} mmol, 39.7%), III (R_f 0.50; 9.0 mg, 4.8×10^{-3} mmol, 18.5%), and unreacted II (R_f 0.30; 5.0 mg, 5.19×10^{-3} mmol, 9.98%) was shown by comparative TLC and IR and ^1H NMR spectroscopy. The base line material was noncrystalline and was not characterized.

Reaction of $[\text{N}(\text{C}_2\text{H}_5)_4][\text{HRu}_3(\text{CO})_{11}]$ with HgI_2 . To a Schlenk tube containing a stirring THF (30.0 mL) solution of mercuric iodide (30.6 mg, 6.74×10^{-2} mmol) was injected a THF (5.0 mL) solution of $[\text{N}(\text{C}_2\text{H}_5)_4][\text{HRu}_3(\text{CO})_{11}]$ (50.0 mg, 6.74×10^{-2} mmol) via syringe. Upon addition of the purple $[\text{N}(\text{C}_2\text{H}_5)_4][\text{HRu}_3(\text{CO})_{11}]$ solution, the reaction mixture turned red-brown and a yellow precipitate began to form within 30 min as the reaction mixture became lighter in color. After 2 h, the supernatant was light orange, and presence of mercury metal along with a copious yellow precipitate was noted. TLC in hexanes and dichloromethane/hexanes (1:4) showed that no mercuric iodide was present, but a faint spot near the solvent front was observed. The precipitate was allowed to settle and the supernatant was removed by cannulation, leaving a yellow amorphous powder and traces of mercury. The residue was stirred with THF (10.0 mL), resulting in a suspension of the fine yellow compound, which was then removed by cannulation. In this manner, the yellow product was separated from the mercury (5 mg, 1×10^{-2} mmol). The yellow precipitate (VI) was first washed with absolute ethanol (5.0 mL) and then with diethyl ether (5.0 mL) and dried under high vacuum (26.1 mg). The yellow product was insoluble in all solvents tried (hexane, toluene, dichloromethane, THF, diethylether, DMF, ethanol, nitrobenzene, nitromethane, Me_2SO , 2-ethoxyethanol, acetone, and water). IR (KBr): 2045 (s), 2000 (s), 1985 (s), 1960 (s) (CO terminal) cm^{-1} . Anal. Calcd for $\text{HgRu}(\text{CO})_4$: C, 11.61; Ru, 24.4; Hg, 48.6. Found: C, 12.67; Ru, 24.4; Hg, 44.10; compound I, 0.00.

Table VI. Final Positional and Anisotropic Thermal Parameters with Their Standard Deviations of

atom	x	y	z	$B(\text{eq}), \text{\AA}^2$
Hg(1)	0.37188 (5)	0.14785 (2)	0.50996 (3)	3.46 (1)
Hg(2)	0.38069 (5)	0.09740 (2)	0.32824 (3)	3.21 (1)
Ru(1)	0.14678 (10)	0.13710 (4)	0.53813 (6)	2.79 (3)
Ru(2)	0.32344 (11)	0.21350 (4)	0.62559 (6)	3.09 (3)
Ru(3)	0.10205 (12)	0.25012 (4)	0.52270 (6)	3.55 (3)
Ru(4)	0.25726 (10)	0.11018 (4)	0.16739 (6)	2.88 (2)
Ru(5)	0.26171 (10)	0.00714 (4)	0.24410 (6)	2.75 (2)
Ru(6)	0.36933 (10)	0.01887 (4)	0.12640 (6)	3.02 (2)
Ru(7)	0.54862 (11)	0.14518 (5)	0.44466 (6)	3.61 (3)
C(71)	0.4766 (15)	0.2100 (8)	0.3903 (9)	4.9 (5)
O(71)	0.4314 (16)	0.2484 (6)	0.3569 (9)	9.1 (6)
C(72)	0.5853 (14)	0.0747 (8)	0.4901 (8)	4.3 (5)
O(72)	0.6061 (13)	0.0330 (6)	0.5168 (7)	6.9 (5)
C(73)	0.6461 (16)	0.1831 (8)	0.5334 (10)	6.0 (6)
O(73)	0.7087 (13)	0.2038 (7)	0.5877 (8)	9.3 (6)
C(74)	0.6600 (16)	0.1383 (7)	0.3838 (9)	5.8 (6)
O(74)	0.7281 (13)	0.1324 (6)	0.3528 (8)	8.6 (5)
C(11)	0.2056 (13)	0.0629 (6)	0.5619 (8)	3.7 (4)
O(11)	0.2290 (12)	0.0185 (4)	0.5709 (7)	6.5 (4)
C(12)	0.1123 (15)	0.1385 (6)	0.4281 (9)	4.3 (5)
O(12)	0.0855 (12)	0.1388 (5)	0.3618 (6)	6.3 (4)
C(13)	-0.0154 (17)	0.1166 (6)	0.5278 (9)	4.7 (5)
O(13)	-0.1105 (12)	0.1006 (6)	0.5221 (9)	7.9 (5)
C(21)	0.4672 (17)	0.1737 (7)	0.6876 (10)	4.8 (5)
O(21)	0.5479 (12)	0.1516 (6)	0.7224 (8)	7.0 (5)
C(22)	0.3418 (15)	0.2681 (6)	0.7023 (9)	4.5 (5)
O(22)	0.3505 (13)	0.3009 (5)	0.7481 (8)	7.9 (5)
C(23)	0.3983 (16)	0.2591 (6)	0.5684 (9)	4.9 (5)
O(23)	0.4438 (14)	0.2868 (5)	0.5373 (8)	8.1 (5)
C(31)	0.1124 (14)	0.3239 (6)	0.5545 (9)	4.4 (5)
O(31)	0.1194 (13)	0.3677 (4)	0.5770 (7)	6.8 (5)
C(32)	-0.0671 (18)	0.2494 (6)	0.4775 (11)	5.7 (6)
O(32)	-0.1721 (14)	0.2466 (6)	0.4521 (9)	8.2 (6)
C(33)	0.1376 (18)	0.2673 (6)	0.4277 (10)	5.7 (6)
O(33)	0.1634 (17)	0.2751 (5)	0.3744 (8)	10.0 (7)
C(1)	0.1337 (12)	0.2046 (5)	0.6451 (7)	2.9 (4)
C(2)	0.1870 (13)	0.1653 (5)	0.6622 (7)	3.2 (4)
C(3)	0.1828 (16)	0.1390 (6)	0.7358 (8)	4.9 (5)
C(4)	0.0532 (20)	0.1241 (10)	0.7298 (12)	9.0 (9)
C(5)	0.2252 (27)	0.1812 (8)	0.8032 (10)	10.1 (9)
C(6)	0.2639 (20)	0.0887 (8)	0.7560 (11)	7.5 (7)
C(41)	0.2050 (15)	0.1389 (6)	0.0653 (9)	4.8 (5)
O(41)	0.1781 (12)	0.1553 (5)	0.0040 (6)	6.7 (4)
C(42)	0.4091 (16)	0.1466 (6)	0.1878 (7)	4.0 (4)
O(42)	0.4971 (11)	0.1715 (5)	0.1981 (7)	6.2 (4)
C(43)	0.1739 (15)	0.1658 (6)	0.2068 (9)	4.4 (5)
O(43)	0.1289 (12)	0.2017 (4)	0.2265 (6)	6.3 (4)
C(51)	0.2093 (13)	-0.0666 (6)	0.2146 (8)	4.0 (4)
O(51)	0.1819 (12)	-0.1096 (4)	0.1976 (8)	6.8 (4)
C(52)	0.1815 (14)	0.0120 (5)	0.3222 (7)	3.6 (4)
O(52)	0.1334 (11)	0.0116 (4)	0.3686 (6)	6.3 (4)
C(53)	0.4208 (15)	-0.0189 (6)	0.3080 (8)	3.9 (4)
O(53)	0.5107 (11)	-0.0357 (5)	0.3437 (7)	6.0 (4)
C(61)	0.5397 (15)	0.0321 (5)	0.1848 (9)	4.0 (5)
O(61)	0.6365 (11)	0.0413 (5)	0.2181 (7)	6.6 (4)
C(62)	0.3841 (14)	0.0428 (6)	0.0311 (8)	4.2 (5)
O(62)	0.3895 (12)	0.0564 (5)	-0.0288 (6)	6.8 (4)
C(63)	0.3908 (14)	-0.0559 (7)	0.1091 (9)	4.2 (5)
O(63)	0.4037 (12)	-0.1008 (5)	0.1004 (7)	6.3 (4)
C(7)	0.1989 (13)	0.0289 (5)	0.1214 (6)	2.9 (4)
C(8)	0.1123 (12)	0.0457 (5)	0.1476 (7)	3.1 (4)
C(9)	-0.0238 (12)	0.0475 (6)	0.1268 (8)	3.8 (4)
C(10)	-0.0717 (16)	-0.0118 (6)	0.1163 (12)	6.8 (7)
C(14)	-0.0769 (14)	0.0752 (7)	0.0459 (9)	5.3 (5)
C(15)	-0.0683 (16)	0.0768 (10)	0.1883 (11)	8.6 (8)

^aThe isotropic equivalent thermal parameters of the anisotropically refined atoms correspond to the expression $B = \frac{1}{3}[a^2B(1,1) + b^2B(2,2) + c^2B(3,3) + ab(\cos \gamma)B(1,2) + ac(\cos \beta)B(1,3) + bc(\cos \alpha)B(2,3)]$.

The original supernatant was concentrated, applied to a preparative chromatography plate, and eluted with dichloromethane/hexanes (1:4) to give one yellow moving band and a red base line. Workup in the usual manner yielded 10 mg of $\text{Ru}_3(\text{CO})_{12}$ identified by comparative TLC and

IR spectroscopy. An IR was taken of the red base line material (22.7 mg). IR: 2085 (s), 2020 (s), 1960 (s) (C≡O, terminal) cm^{-1} .

This reaction was repeated with 2 and then 3 equiv of mercuric iodide. In these subsequent experiments, a similar amount of the yellow product (28.3 and 31.5 mg) and base line was obtained but no $\text{Ru}_3(\text{CO})_{12}$ was detected with 2 or more equiv of mercuric iodide. Approximately 10 mg of mercury was obtained with 2 equiv, but with 3 equiv a significantly larger amount of mercury was precipitated (40 mg).

Reaction of I with *cis*-Ru(CO)₄(HgI)₂. Compound I (18.5 mg, 1.81×10^{-2} mmol) was dissolved in CD_2Cl_2 (1.0 mL). The ^1H NMR spectrum showed a singlet resonance at 1.28 ppm. *cis*-Ru(CO)₄(HgI)₂ (5.1 mg, 6.26×10^{-3} mmol) was added and a ^1H NMR spectrum was taken. ^1H NMR (CD_2Cl_2): 1.50 (s, IV); 1.36 (s, III); 1.34 (s, II); 1.27 ppm (s, residual I) ppm. Comparative TLC of the reaction mixture with known samples of IV, III, and II is consistent with these assignments.

Equilibrium Constant Determinations. A solution of the unsymmetrical mercuric compound, AHgB , [where $\text{A} = \text{Ru}_3(\text{CO})_9(\mu_3\text{-C}_2\text{-}t\text{-Bu})^-$, and $\text{B} = \text{I}^-, \text{Br}^-$] was prepared by weighing approximately 20 mg of the solid material into a 1.00-mL volumetric flask and filling it to the mark with CDCl_3 . A volume of this solution (0.20 mL) was then diluted with CDCl_3 to 1.00 mL in an NMR tube and sealed under nitrogen.

^1H NMR spectra were recorded periodically at 300 K as the redistribution reaction approached equilibrium. It took 28–31 days to reach equilibrium. As the reaction proceeded, the new peak of the symmetric mercuric compound, HgA_2 , grew progressively as the original unsymmetrical compound peak diminished. When no further change in the integration ratio of the symmetric to the unsymmetrical mercuric compound was observed, the reaction was assumed to be at equilibrium.

In a typical experiment with II, 11.5 mg of the compound was dissolved in 10.0 mL of CDCl_3 to give a 1.19×10^{-2} M solution. An aliquot of this solution, 0.20 mL, was diluted to 1.0 mL with CDCl_3 . ^1H NMR spectra were recorded daily until the integration of IV to II remained constant. A similar procedure was used in the case of $\text{BrHgRu}_3(\text{CO})_9(\mu_3\text{-C}_2\text{-}t\text{-Bu})$ (IIa). The results are shown in Tables III and IV.

Promotion of the Redistribution Reaction by Ru_3 Clusters. To investigate the promotion of the redistribution of II to IV, samples of (II) were prepared with increasingly larger concentrations of added $\text{Ru}_3(\text{CO})_{12}$. In one experimental run, the concentration of II was 2.38×10^{-3} M initially. The initial concentrations of $\text{Ru}_3(\text{CO})_{12}$ and the calculated concentrations of IV are listed in Table V. ^1H NMR spectra were recorded after 1-h reaction time. The concentration of the symmetric species, IV, was determined from the integration ratio. Figure 3 shows a plot of [IV] vs. [$\text{Ru}_3(\text{CO})_{12}$].

X-ray Diffraction Data

An orange crystal of III (ca. $0.25 \times 0.28 \times 0.11 \text{ mm}^3$) selected for data collection was mounted on the end of a thin glass fiber with the face diagonal of the crystal (101) approximately parallel to the fiber axis. A total of 15 randomly selected reflections in the range $12^\circ < 2\theta < 25^\circ$ were accurately centered and indexed on a Nicolet/Syntex P_2 automated diffractometer equipped with graphite monochromator and Mo $\text{K}\alpha$ radiation ($\lambda = 0.71069 \text{ \AA}$). *cis*-Ru(CO)₄[HgRu₃(CO)₉(C₂-*t*-Bu)]₂, $M_r = 1887.2$, crystallizes in the monoclinic space group $\text{P}2_1/n$ [No. 14, C_{2h}^2]¹⁷ with $a = 11.534(8) \text{ \AA}$, $b = 24.456(8) \text{ \AA}$, $c = 18.160(5) \text{ \AA}$, $\beta = 108.05(4)^\circ$, $V = 4870(4) \text{ \AA}^3$, $Z = 4$, $\mu(\text{Mo K}\alpha) = 84.19 \text{ cm}^{-1}$, $d_{\text{calcd}} = 2.574 \text{ g cm}^{-3}$, $d_{\text{measd}} = 2.564 \text{ g cm}^{-3}$ by neutral buoyancy in $\text{CCl}_4/\text{CHBr}_3$.

(17) Space group $\text{P}2_1/n$ is an alternative, nonstandard setting of $\text{P}2_1/c$ (No. 14) with the following equivalent positions: (x, y, z) ; $(-x, -y, -z)$; $(1/2 + x, 1/2 - y, 1/2 + z)$; $(1/2 - x, 1/2 + y, 1/2 - z)$.

A total of 9106 intensity data were collected in the $hk\pm l$ quadrant of reciprocal space by using the $\omega/2\theta$ scan technique out to a 2θ maximum of 50° . The scan speed was varied between 2.55 and $29.3^\circ \text{ min}^{-1}$, depending on the intensity, with the ω scan width given by $[2.0 + \Delta(\alpha_1 - \alpha_2)]^\circ$. During the course of data collection the intensities of three standard reflections (048; $\bar{1}84$; 0,10, $\bar{2}$) monitored for crystal and instrumental stability were sampled after every 100 intensity measurements and found to be satisfactory. The intensity data were corrected for absorption¹⁸ and Lorentz polarization effects and merged to yield 8626 unique reflections [$R_{\text{int}} = \sum(F_o^2 - \langle F_o^2 \rangle) / \sum F_o^2 = 0.034$]. Of these, 5586 observations with $F_o^2 > 3\sigma(F_o^2)$ were used in the structure solution and refinement.

The solution of the structure was obtained by direct methods¹⁹ that revealed the position of Hg and Ru atoms. All remaining non-hydrogen atoms were located in subsequent structure factor/difference Fourier steps. Full-matrix least-squares refinement²⁰ minimizing the quantity $\sum w|F_o| - |F_c|^2$, with all non-hydrogen atoms assigned anisotropic thermal parameters, led to final residual indices $R_F = 0.045$, $R_{wF} = 0.049$ ($R_F = 0.075$, $R_{wF} = 0.054$ for all data), and $\text{GOF} = 1.46$.²¹ No attempt was made to locate the hydrogen atoms of the molecule. A final difference Fourier map showed no peaks $> 0.71 \text{ e/\AA}^3$, these being ca. 1 \AA from the Hg(2) atom of the molecule. The neutral scattering factors used for all atoms, including anomalous dispersion corrections for Hg and Ru atoms, were obtained from standard sources.²² The final atomic coordinates and the equivalent isotropic thermal parameters are given in Table VI.

Acknowledgment. We gratefully acknowledge support of this research by the donors of the Petroleum Research Fund, administered by the American Chemical Society, and the National Science Foundation (Grant No. CHE 8412047). We also thank Professor Robert Bau for use of his Syntex diffractometer and Dr. David A. Miller for help with the neutron activation analyses.

Registry No. I, 76741-75-8; II, 74870-35-2; IIa, 74870-34-1; III, 99593-31-4; III-¹³C₄, 99604-50-9; IV, 84802-26-6; V, 57673-31-1; VI, 99582-68-0; $\text{Ru}_3(\text{CO})_{12}$, 15243-33-1; $[\text{N}(\text{C}_2\text{H}_5)_4][\text{HRu}_3(\text{CO})_{11}]$, 12693-45-7; $\text{Na}_2\text{Ru}(\text{CO})_4$, 57398-60-4; HgI_2 , 7774-29-0; $[\text{As}(\text{C}_6\text{H}_5)_4]_2\text{Ru}(\text{CO})_4$, 99582-69-1; HgBr_2 , 7789-47-1.

Supplementary Material Available: Complete listings of final positional and anisotropic thermal parameters, bond distances and angles, and observed and calculated structure factors (46 pages). Ordering information is given on any current masthead page.

- (18) Empirical absorption correction was made by using the ψ -scan technique.
- (19) MULTAN: A system of computer programs for the automatic solution of crystal structures from x-ray diffraction data (Germain, G.; Main, P.; Woolfson, M. M.; *Acta Crystallogr., Sect. A: Cryst. Phys., Diffraction, Theor. Gen. Chem.* **1971**, *A27*, 368).
- (20) Due to storage limitations, the molecule was refined in two separate matrices. The molecule was split into two equal units each containing the $\text{Ru}(\text{CO})_4$ fragment and a $\text{HgRu}_3(\text{CO})_9(\mu_3\text{-C}_2\text{-}t\text{-Bu})$ unit. The positional and thermal parameters of each unit were refined simultaneously. Major computations in this work were performed on the CSUN CDC CYBER 170/750 computer with CRYSYS, an amalgamated set of local crystallographic programs.
- (21) $R_F = \sum(|F_o| - |F_c|) / \sum F_o$, $R_{wF} = [\sum w(|F_o| - |F_c|)^2 / \sum wF_o^2]^{1/2}$, $w = 4F_o^2 / (\sigma^2(F_o^2) + (pF_o^2)^2)$, with $p = 0.04$ and $\sigma(F_o^2)$ based on counting statistics alone, and $\text{GOF} = [\sum w(|F_o| - |F_c|)^2 / (N_o - N_v)]^{1/2}$, where $N_o = 5586$ and $N_v = 253$ are the number of observations and the number of variables, respectively.
- (22) "International Tables for X-Ray Crystallography"; Vol. IV, Kynoch Press: Birmingham, England, 1974; Vol. IV.